Crosslinking and composition influence the surface properties, mechanical stiffness and cell reactivity of collagen-based films.

Chloe N. Grover[a], Jessica H. Gwynne[a], Nicholas Pugh[b], Samir Hamaia[b], Richard W. Farndale[b], Serena M. Best[a] and Ruth E. Cameron[a]

[a] Department of Materials Science and Metallurgy, Cambridge Centre for Medical Materials, University of Cambridge, Pembroke Street, Cambridge CB2 3QZ, UK
[b] Department of Biochemistry, University of Cambridge, Downing Site, Cambridge, CB2 1QW, UK.

Corresponding Author: Chloe N. Grover, Department of Materials Science and Metallurgy, Cambridge Centre for Medical Materials, University of Cambridge, Pembroke Street, Cambridge CB2 3QZ, UK. Telephone: +44 1223 362966, Fax: +44 1223 334366. Email: cng21@cam.ac.uk

Abstract

This study focuses on determining the effect of varying the composition and crosslinking of collagen-based films on their physical properties and interaction with myoblasts. Films composed of collagen or gelatin and crosslinked with a carbodiimide were assessed for their surface roughness and stiffness. These samples are significant because they allow variation of physical properties as well as offering different recognition motifs for cell binding. Cell reactivity was determined by the ability of myoblastic C2C12 and C2C12-α2+ cell lines (with different integrin expression) to adhere to and spread on the films. Significantly, crosslinking reduced the cell reactivity of all films, irrespective of their initial composition, stiffness or roughness. Crosslinking resulted in a dramatic increase in the stiffness of the collagen film and also tended to reduce the roughness of the films ($R_q = 0.417 \pm 0.035$ μm, $E = 31 \pm 4.4$ MPa). Gelatin films were generally smoother and more compliant than comparable collagen films ($R_q = 7.9 \pm 1.5$ nm, $E = 15 \pm 3.1$ MPa). The adhesion of α2-positive cells was enhanced relative to the parental C2C12 cells on collagen compared with gelatin films. These results indicate that the detrimental effect of crosslinking on cell response may be due to the altered physical properties of the films as well as a reduction in the number of available cell binding sites. Hence, although crosslinking can be used to enhance the mechanical stiffness and reduce the roughness of films, it reduces their capacity to support cell activity and could potentially limit the effectiveness of the collagen-based films and scaffolds.

Keywords films; crosslinking; cell adhesion; electron microscopy; atomic force microscopy

1. Introduction

Research on biomaterial scaffolds for use in soft tissue engineering reflects their ability to deliver cells whilst acting as a mechanical support [1-5]. Despite the widespread use of scaffolds composed of extracellular matrix proteins [4, 6-9], detailed analysis of their properties at a cellular lengthscale has not been carried out; in particular the effect of composition and crosslinking on stiffness, surface roughness and ability to support cell activity. Previous studies have concentrated on assessing the individual effect of different compositions and methods of crosslinking on cell activity [10, 11] or on physical properties [12-15]. However, comparison of the physical properties and cell reactivity of films of different compositions before and after crosslinking has not yet been performed. The prior research has indicated that crosslinking, using a carbodiimide system, is an effective way of increasing the mechanical stiffness and degradation resistance of biomaterials without being cytotoxic. However, carbodiimide treatment of biomaterials: the formation of crosslinks between free amine groups, typically on lysine residues, and free carboxylate anions, typically on glutamate (E) or aspartate (D) residues, will reduce the availability of cell-binding sites on scaffold proteins, but knowledge of this direct effect of crosslinking on the cell activity of biomaterial thin films is incomplete. The importance of this question arises from the crucial role of such glutamate or aspartate residues in the collagens or other matrix molecules in binding to the relevant integrin cell surface receptors [16, 17].

This research addresses the effect of altering the crosslinking of films on their physical properties and cell reactivity. In particular, we have studied collagen and gelatin, proteins commonly used in soft tissue engineering, to compare the effect of alteration of the protein structure, and thus available cell binding sites, on the physical properties and cell reactivity of films. GXOGEX' motifs in triple-helical collagen interact with cells via specific integrins, notably $\alpha_2\beta_1$, and heat-denaturation of collagen, to produce gelatin, destroys the ordered three-dimensional triple-helical structure, leaving, after cooling, a mixture of mis-aligned triple helices, peptide fragments and random coils, unable to fully assemble and form ordered fibrils [18, 19]. This process alters the adhesive cues presented to cells, with GXOGEX' motifs in the native collagen interacting with myoblast cell lines via the collagen-binding β_1 integrins, and denatured collagen interacting via exposed RGD adhesion molecules which can signal to other integrins, such as $\alpha_5\beta_1$ and $\alpha_V\beta_3$ [20-25].

Our research has been focused on myocardial regeneration; therefore we have investigated interactions with mouse myoblast cells lines. Two different myoblast cell lines were used,

C2C12 and C2C12-α2+, to explore the effect of altering the available integrins on cell binding. C2C12 cells are known to express no endogenous collagen-binding integrins but can interact via the RGD-recognising integrins such as $\alpha_V\beta_3$ and $\alpha_5\beta_1$ [26], whereas the α_2-transfected cell line, C2C12-α2+, expresses in addition, the collagen-binding integrin $\alpha_2\beta_1$ [27-28]. In investigating both collagen and gelatin we expect to be able to generate samples with a range of values for surface roughness, mechanical stiffness and available cell binding sites, with which to explore the effect of crosslinking on the bioactivity of the films. Varying receptor expression, using the different cell types, provides additional information on the cell binding. However, although myocardial cells are used in this paper, these proteins are not limited to myocardial application and can be used to produce cost-effective films and scaffolds for a variety of devices such as in osteo-chondral repair, dermal replacement and cartilage [4, 10, 29-31].

Films were prepared and characterised in terms of their physical properties and cellular interactions. Thin films are a model for the struts of bulk scaffolds and provide information on the properties of these devices at a cellular lengthscale. The study of the properties of thin films including the surface roughness and mechanical stiffness, as well as their ability to interact with cells, can indicate the suitability of biomaterials for use in tissue engineering [21, 32]. Scanning Electron Microscopy (SEM) and Atomic Force Microscopy (AFM) were used to characterise the film microstructure and surface roughness, while measurements of Young's modulus was used to assess the effect of composition and crosslinking on mechanical properties. The adhesion of C2C12-α2+ and C2C12 cells on different films and surfaces was studied. Calculation of the cell surface coverage as well as morphological analysis of the cells grown on films for up to three days was performed. This approach enables an investigation of the effects of crosslinking and composition on the surface roughness, mechanical properties and cell activity of collagen-based films.

2. Materials and Methods

2.1 Film Fabrication

In total, six different collagen-based films were prepared by drying a suspension of protein on either Teflon sheets or in 24-well plates. Films were prepared from either a collagen slurry, gelatin suspension or mixed collagen-gelatin suspension (ratio 1:1). Briefly, a suspension containing 0.5% (w/v) collagen (bovine dermal type I, DevroMedical) was swollen overnight in 0.05 M acetic acid at 4 ± 2°C. The resulting suspension was homogenised on ice for 10 min at 9,500 rpm using an Ultra-Turrax VD125 (VWR International Ltd, UK). Air bubbles were removed from the suspension by centrifuging at 2,500 rpm for 5 min (Hermle Z300, Labortechnik, Germany).

Gelatin-based suspensions could not be prepared by homogenisation. Dissolution of the powder required heating and homogenisation at high temperatures resulted in the formation of a foam. However, the solution began to gel at temperatures below approximately 15°C, so homogenisation could not be carried out at low temperatures either. Gelatin-based solution, 0.5% (w/v), was instead prepared by dissolving gelatin (bovine skin type B, Sigma-Aldrich) in 0.05 M acetic acid at 37–45ºC with stirring for 1 h. The solution was then cooled to room temperature with stirring. The mixed collagen-gelatin suspension was prepared by mixing a gelatin solution with a collagen slurry (both 0.5% w/v), before centrifuging.

The protein suspensions were then dried overnight on a Teflon sheet at room temperature in a laminar flow hood. This process produces a thin film of protein, with an average thickness of 15 μm.

2.2 Chemical Crosslinking

After drying, crosslinking was carried out using 1.150 g 1-ethyl-3-(3-dimethylaminopropyl) carbodiimide hydrochloride (EDAC) and 0.276 g N-hydroxy-succinimide catalyst (NHS, both Sigma-Aldrich) per gram of film as previously described [33]. The crosslinking solution was prepared in 75% ethanol/water (v/v) [5, 34]) and the samples were crosslinked for 2 h (pH 5.5). After crosslinking the films were washed twice in 75% ethanol, followed by three times in deionised water for 30 min each. The crosslinked films were allowed to dry overnight in a fume hood.

2.2.1 Films for AFM

Films for AFM were dried directly onto glass coverslips and crosslinked in situ.

2.2.2 Films for Cell Culture

To produce films for cell culture, slurries 0.5% (w/v) were added to 24-well tissue culture wells (400 µl per well) and dried in a tissue culture hood overnight. Films were then crosslinked in situ.

2.3 Amino acid analysis

For amino acid analysis, collagen and gelatin samples were hydrolysed with 6 M HCl for 22 h at 115°C, dried under vacuum and dissolved in 10 mM HCl. The amino acid mixture was analysed using a Biochrom 30 instrument and quantified using Chromeleon software at the Department of Biochemistry, Cambridge.

2.4 Determination of Primary Amine Group Content and Degree of Crosslinking

The degree of crosslinking can be estimated from the residual amount of free amine groups of (non-) crosslinked samples. The concentration of free primary amine groups ($-NH_2$) present in the initial non crosslinked and the crosslinked films was determined using a 2, 4, 6-trinitrobenzenesulfonic acid (TNBS, Sigma-Aldrich) assay with a protocol similar to those reported by Sashidar *et al.* and Ofner *et al.* [35, 36]. To each sample (1−3 mg) 0.5 ml of a 4% (w/v) NaHCO3 solution and 0.5 ml of a freshly prepared solution of 0.05% (w/v) TNBS was added. After reaction for 2 h at 40°C, 1.5 ml of 6 M HC1 was added and the samples were hydrolysed at 60°C for 90 min. The reaction mixture was diluted with distilled water (2.5 ml), cooled to room temperature and the absorbance at 320 nm (A_{320}) was measured using a Fluostar Optima spectrophotometer. Controls (blank samples) were prepared using the same procedure, except that HCl was added prior to the TNBS solution. The absorbance of the blank samples was subtracted from each sample absorbance. The absorbance was correlated to the concentration of free amino groups using a calibration curve obtained with glycine in an aqueous $NaHCO_3$ solution (0.1 mg/ml).

The experiment was repeated three times and the average, along with the standard error, was calculated. The non-crosslinked sample was assumed to contain 100% of the available free amine groups and this value was used to calculate the percentage of remaining free amine groups after the crosslinking treatment.

2.5 SEM

SEM was used to analyse the film surface and cross-sectional structure. Films were mounted on stubs and sputtered with an ultrathin layer of platinum for 20 s at 20 mA, in an SEM coating system. Both film surfaces and the cross-section were studied with a JEOL JSM-820 scanning electron microscope operating at 10 kV for low magnification, and a JEOL 6340F FEGSEM operating at 5 kV for high magnification images. Gelatin fibre bundle diameters were measured from the SEM images of the film cross-section.

2.6 AFM

The AFM apparatus (Dimension 3100) was operated in light tapping mode, using standard tapping probes (RTSEP Silicon AFM tips, Veeco: resonant frequency 200−400 Hz, spring constant 20−40 N/m) under ambient conditions (dry samples). All image analysis was carried out using WSxM software [37].

Root mean square (RMS) roughness (R_q) was measured for five different locations on each film: image size 50 x 50 μm, scan rate of 0.2 Hz and 256 samples/line. Images were first flattened (offset) and then the average roughness of four 20 x 20 μm squares (randomly distributed within the image) was measured. Collagen fibre-bundle diameter was measured from fibres visible in 20 x 20 μm images. The periodic repeat of the banding pattern on collagen fibres was measured by drawing a line profile on a parabolic flattened image and measuring the distance between at least four peaks. Averages of 10−20 measurements for fibre size and 4−5 measurements for banding repeat were taken.

2.7 Mechanical Testing

Uniaxial tensile testing was used to determine the effect of composition and crosslinking on the modulus of the films. Mechanical testing of films was carried out using a Hounsfield tester equipped with a 5 N load cell and specially designed testing apparatus (Figure 1). Film samples used for mechanical testing were first cut into rectangular strips, 7 mm wide by 45–70 mm long (n = 14 per group), using a scalpel. Samples were pre-hydrated in water for 30 min before measuring the thickness at three different areas; testing was then carried out in a bath of water. Samples were clamped in a horizontal position, gauge length 10 mm, and testing was conducted at a constant extension rate of 6 mm min^{-1}. All samples were stretched until failure and data was used to plot a stress-strain curve. The tensile modulus (E) was defined as the slope of a tangent to the curve at 5 % strain, 20 % strain and high values of strain (where the maximum gradient was reached).

Hydration of non-crosslinked films made them difficult to handle and significantly weaker. Tensile testing could only be performed on non-crosslinked collagen films as all other compositions were too weak to handle when hydrated.

2.8 Cell Culture

C2C12 and C2C12-α2+ mouse myoblast cells were a gift from Prof D. Gullberg, University of Bergen, Norway, where C2C12 is the parental cell line and C2C12-α2+ is a stably transfected cell line (with the human integrin α_2 subunit). Cells were cultured in T−75 flasks (nunc) using Dulbeccos Modified Eagle Medium (DMEM, Invitrogen) supplemented with 10% FBS (Invitrogen), 1% L-glutamine and 2% penicillin/streptomycin (Sigma). Before seeding, cells (passage 2−3) were detached using trypsin (Invitrogen) and spun down to a pellet. All films were rinsed three times with sterile phosphate buffered saline (pH 7.4, Invitrogen) and pre-incubated with DMEM for 30 min at 37°C.

A study was conducted using C2C12-α2+ cells marked using CellTracker Green (CMFDA, Invitrogen) to enable measurement of the degree of cell spreading and surface coverage. Cells were re-suspended in 1 ml CellTracker stock (10 μM) made up in DMEM and incubated with rocking for 60 min at 37°C. The suspension was then centrifuged at 403 g for 5 min (Geneflow) and washed in DMEM. This was repeated and cells were then suspended in supplemeted DMEM for use in culture. Cells were then seeded on films in 24-well plates, in triplicate, at a density of 2000 cells/well in 800 μl DMEM and placed in an incubator for up to 72 h at 37ºC under 5% CO_2. After 1, 24 and 72 h cells were imaged as detailed in the next section.

To compare the interaction of films with specific integrins both C2C12-α2+ and C2C12 cells were used. The films were seeded with either C2C12-α2+ or C2C12 cells, in triplicate, at a density of 1000 cells/well in 800 μl DMEM and then placed in an incubator for 72 h at 37 ºC under 5% CO_2.

2.9 Hoechst-Propidium Iodide Assay

Cells were visualised for counting and morphometry using the stains Hoechst 33258 and propidium iodide (PI) (Sigma-Aldrich). A working solution of the dyes was prepared, and after the specified incubation time, the working solution was added to each well to give a final concentration of 4 μg/ml Hoechst and 1 μg/ml PI. This was incubated for 15 min at 37ºC and the fluorescence was then measured on two channels (Hoechst: excitation 355 nm; emission

461 nm and PI: excitation 535 nm; emission 617 nm) with an additional channel for CellTracker fluorescence of the time point study (excitation 492 nm; emission 517 nm) using a fluorescence spectrophotometer (AF6000 LASAF confocal microscope). Four images were taken from the centre of each well and analysed using ImageJ software (NIH, USA) for live and dead cell count, surface coverage (the percentage of the surface covered with cells), individual cell area and aspect ratio (longest dimension / shortest dimension).

2.10 Real Time Cell Adhesion Assay

The xCELLigence system (Roche Diagnostics, UK) allows continuous measurement and quantification of cell adhesion and spreading in real time. It measures the electrical impedance across a microelectrode array on specialized 96-well 'E-plates' [38]. The increase in impedance as cells contact or spread over the surface is reported as a dimensionless parameter, the Cell Index. This method has been used previously to report the adhesion of cells or platelets as they contact and spread on wells coated with adhesive substances [39, 40].

Two separate studies were conducted. The first was to determine if binding to GFOGER (a type I collagen peptide sequence) was dependent on the presence of the integrin $\alpha_2\beta_1$, and the second was to confirm that the binding of C2C12 parent and α2-positive cells to gelatin is via RGD-binding integrins. The anti-β3 integrin (anti-β3) monoclonal antibody was from BD Biosciences (Cat 550541, Oxford, UK), while the RGD blocking peptide, cyclic-RGD (c-RGD), was from Bachem (Cat H-2672, Switzerland). The GFOGER specific triple-helical peptide was synthesized, purified, and verified as previously described [41, 42].

E-plates were coated in triplicate with 100 µl per well of GFOGER peptide or bovine serum albumin (both 10 µg/ml in 0.01 M acetic acid), for at least 1 h at 20°C. Excess ligand was discarded, and the wells were blocked with 175 µl of 5% BSA (50mg BSA in 1 ml PBS) PBS for 1 h at 20°C. Plates were washed three times with 175 µl PBS per well. Fifty microlitres of PBS containing 1 mM Mg^{2+} or EDTA (to enhance or inhibit integrin extracellular domain binding [41]) were added to each well and allowed to equilibrate at 37°C, and baseline impedance measurements were recorded. Fifty microlitres of C2C12 or C2C12-α2+ cells suspended in PBS containing 1 mM Mg^{2+} or EDTA (40×10^4 cells/ml) were then added to give a final cell count of 20,000 cells per well. Impedance was recorded every 30 s for 2.5 h. A similar protocol was followed for the RGD-peptide blocking study. E-plates were coated with 100 µl per well of gelatin protein (100 µg/ml in 0.01 M acetic acid) or BSA for at least 1 h at 20°C. After blocking with 5% BSA and washing with PBS, 50 µl of PBS containing

1 mM Mg^{2+} or EDTA were added to each well and allowed to equilibrate at 37°C, and baseline impedance measurements were recorded. C2C12 and C2C12-α2+ cells were pre-incubated with c-RGD (10 μg/ml) or anti-β3 (10 μg/ml) 15 min before addition to the wells. Fifty microlitres of non-treated or pre-incubated cells, suspended in PBS containing 1 mM Mg^{2+} or EDTA (40 x 10^4 cells/ml) were then added to give a final cell count of 20,000 cells per well. Impedance was recorded every 30 s for 2.5 h.

2.11 Statistical Analysis

Results are expressed in the figures as mean ± standard error. Student's t-test was used to compare the roughness and modulus of films, and two-way analysis of variance was used to evaluate the effects of crosslinking and composition on the cellular attachment. Crosslinked samples were compared with non-crosslinked samples of the same composition and a significant difference of $p \leq 0.05$ was denoted by *. Additionally, different composition were compared and a ■ indicates significant difference between compositions for statistical significance of $p \leq 0.05$.

3. Results

3.1 Amino acid analysis and free amino group content

The amino acid analysis shows similarities in the collagen and gelatin samples, with gelatin having a slightly higher lysine content (Supplementary Data Figure 1). The reaction of TNBS with the primary amino groups in the proteins is used to determine the number of free amino groups in the film samples. The degree of crosslinking is the difference between the chemically determined number of uncrosslinked groups (free amines) before and after crosslinking. In determining the degree of crosslinking, it has been assumed that each lost amine group participates in one cross-link.

The assay values of free amine groups per gram of material before and after crosslinking are recorded in Table 1 (units are in moles of free amine per gram of material x 10^5). Non-crosslinked gelatin has a higher number of free amine groups compared with collagen samples (23 ± 14 x10^{-5} mol/g compared to 14 ± 2.8 x 10^{-5} mol/g). After crosslinking, the free amino group content of all samples decreased significantly, suggesting that the crosslinking procedure is successful. The value of free amine groups in all samples after crosslinking is in the range of 4−9 x10^{-5} mol/g. The degree of crosslinking of gelatin was highest at 82 ± 8%, compared with collagen at 49 ± 2%.

3.2 Effect of Composition on Surface Structure

Scanning Electron Microscopy and Atomic Force Microscopy were used to compare the surface structure and properties of films of different compositions and crosslinking. The cross-section of collagen films showed aligned fibre bundles within the plane of the film, with gelatin films showing a finer scale microstructure (Figure 2). The SEM surface images showed that gelatin-based films had a much smoother surface, whilst those based on collagen were rougher (Supplementary Data Figure 2). This was quantified by AFM, showing the average change in surface height (h) and RMS roughness (R_q) of the collagen-based films was greater than that of gelatin films (Figure 3 and 4, Coll nX h = 3.2 μm, $R_q = 0.4176 \pm 0.035$ μm; Gel nX h = 266 nm, $R_q = 7.9 \pm 1.5$ nm). AFM and SEM image analysis indicated that collagen fibre bundles were larger than gelatin fibre bundles: diameter 0.82 ± 0.16 μm and 0.18 ± 0.28 μm respectively. The height and roughness of mixed collagen-gelatin films was intermediate between the pure films (h = 727 nm, $R_q = 147 \pm 30.5$ nm). The effect of crosslinking was to reduce the roughness of the film surface (Figure 3 and 4). The roughness of dry samples was measured, and although it may be expected for the roughness to change

after hydration, the same trends are likely to apply i.e. collagen films are generally rougher owing to the presence of large fibres compared with relatively smooth gelatin films.

The presence of collagen in all collagen-containing films could be confirmed by identifying its characteristic periodic banding pattern along the fibre (Figure 5). Individual fibres crossed over each other and therefore it was often difficult to find numerous fibres that showed banding along the whole of their length. Fibre diameter was calculated from measurements from up to 20 fibres in each sample, showing an average diameter of 238 ± 29 nm regardless of the composition or crosslink status. An average of 64.4 ± 2.91 nm was calculated for the periodic banding of collagen for all films containing collagen (both non- and crosslinked). These results showed altering the composition or crosslink status had no effect on the collagen fibril size or banding pattern. Gelatin films did not show this banded structure.

3.3 Effect of Composition and Crosslinking on Mechanical Properties

Crosslinking of collagen films using EDAC and NHS was found to result in increased strength. Stress at failure increased twenty-fold and the Young's modulus increased five-fold for crosslinked collagen film compared with non-crosslinked film (Coll nX $\sigma_f = 0.54 \pm 0.23$ MPa, $E = 5.66 \pm 0.34$ MPa; Coll XL $\sigma_f = 11 \pm 3.6$ MPa, $E = 31 \pm 4.4$ MPa, Figure 6). All other non-crosslinked films were too weak to be tested in tension.

Gelatin film has reduced mechanical properties compared with collagen film (Gel XL $\sigma_f = 1.56 \pm 0.19$ MPa, $E = 15 \pm 3.1$ MPa) and the combination of gelatin and collagen resulted in a film with stiffness most similar to that of pure gelatin films ($E = 16 \pm 0.77$ MPa).

3.4 Effect of Composition and Crosslinking on Cell Number, Surface Coverage and Area

Figure 7 show phase contrast and immunofluorescence images of cells seeded on representative gelatin films both non- and crosslinked. It is apparent that the cell number and surface coverage is highest on non-crosslinked films, with a reduced live cell count, increased proportion of dead cells and lower surface coverage after crosslinking. Further analysis of these images using ImageJ software enabled live cell count, surface coverage, cell area and aspect ratio to be determined and are detailed in Figure 8. The number of live cells on the films was found to vary with both composition and crosslinking (Figure 8). The C2C12-α2+ cells showed a significantly lower live cell number and surface coverage when seeded on collagen films than when seeded on gelatin films ($p \leq 0.05$). The lowest cell surface coverage

was seen on the mixed composition films (< 20% of the total area), and the effect of crosslinking was to reduce the cell number and surface coverage of films ($p \leq 0.05$). In particular, crosslinked collagen and gelatin films showed over a 50% decrease in cell number compared with the corresponding non-crosslinked films. Additionally, the percentage of dead cells was higher on crosslinked samples as follows: collagen from 0% dead cells non-crosslinked to 42% with crosslinking, collagen-gelatin from 7% to 33% and gelatin from 2% to 10%.

The degree of C2C12-α2+ cell spreading was quantified by measuring the average cell area and aspect ratio of cells (Figure 8 b and d). The area and aspect ratio of cells was similar on all non-crosslinked films of different compositions. However, the spreading of cells was found to decrease significantly when seeded on crosslinked collagen-containing films (with a more rounded morphology, aspect ratio closer to 1), but there was no difference seen in those cells seeded on pure gelatin films. The same trend was observed at 1, 24 or 72 hours, although, as expected, the cell number and area increased over the three days of culture (results only displayed for 72 hour data).

Figure 9 showed both cell lines to have a higher cell count on gelatin-based films and that crosslinking had a detrimental affect on the cell number regardless of the cell line. The C2C12-α2+ cells showed a higher cell count on pure collagen films compared with C2C12 cells, but there was no significant difference between the cell lines when seeded onto gelatin-containing films (Figure 9). There was an approximate three-fold increase in cell number of C2C12-α2+ cells on collagen compared with C2C12 cells.

3.5 Real-time Cell Adhesion and Spreading

Adhesion of cells on wells coated with adhesion substrates was measured in real time for 2.5 h with the xCELLigence system (results plotted for initial adhesion: up to 1 h). Baseline responses caused by the settling of cells on BSA were indistinguishable. Figure 10 a) shows that there was a strong Mg^{2+}-dependent response of C2C12-α2+ cells to GFOGER compared to that of C2C12 cells, with the response of C2C12 cells only slightly exceeding the EDTA-inhibited cells and control BSA-coated wells. This indicates that the α2-positive cells interact strongly with a collagen-derived peptide, relative to the parent cell line. This Mg^{2+}-dependent adhesion occurs via the specific collagen-binding integrin, $\alpha_2\beta_1$.

Both cell lines showed a strong, magnesium-dependent response to gelatin (Figure 10 b), with

the cell index increasing rapidly over the first hour. This response was reduced significantly and blocked by the pre-incubation of cells with c-RGD or anti-β_3 antibody, indicating that this binding is mediated by RGD-binding integrins expressed by this cell line (such as $\alpha_V\beta_3$ and $\alpha_5\beta_1$). Using c-RGD (10 μg/ml), binding to gelatin could be blocked completely, with no difference in the response to EDTA-inhibited samples or BSA controls. This indicates that adhesion of cells must occur via the interaction of RGD-binding integrins.

4. Discussion

The aim of this study was to determine the effect of composition and crosslinking on the physical properties; surface roughness and mechanical stiffness, as well as on the cellular behaviour of thin films. The use of thin films to characterise properties at a cellular level enables quick and easy pre-screening of biomaterials [21, 32]. As our research interest is in myocardial repair we used myoblasts in our cell activity studies. However, these characterised films could be used to model other cellular interactions using different cell types and for other tissue engineering applications such as dermal repair [10, 12, 30]. Our experiments have demonstrated that by using collagen fibres and gelatin, singly and in combination, and with or without chemical crosslinking, a wide range of surface topographies, mechanical properties and cellular activities can be attained. Collagen-based films had rougher surfaces than gelatin-based films and also a higher modulus when tested in tension. Crosslinking using EDAC and NHS resulted in films with a reduced roughness and was required to introduce mechanical strength and stiffness to the films, as indicated in previous studies [12, 15, 33, 43]. When cells were seeded on these films, the crosslinked films showed decreased cell number and surface coverage when compared to the non-crosslinked films, and there was preferential attachment of α_2-positive cells to collagen compared with the parental cell line.

The degree of crosslinking of the films was assessed using a TNBS assay, where the values for collagen and gelatin samples were comparable with those previously found [35, 44−47]. The free amino group content decreased more significantly for gelatin-based films after crosslinking, indicating that the degree of crosslinking is higher in gelatin than in collagen samples. The denser microstructure of the gelatin films (Figure 2) may lead to increased crosslinks: EDAC forms “zero-length” crosslinks and thus is limited to crosslinking molecules that are directly adjacent or close to each other (1nm) [48, 49]. It should also be noted that the swelling of gelatin in aqueous solution may lead to a more complete TNBS reaction, giving a higher recorded value for the number of free amine groups before crosslinking. Crosslinking, however, is known to reduce the swelling of gelatin [35] and therefore may result in reduced TNBS-reactivity for this reason, as well as by consuming free amino group.

In this study we wished to establish the effect of composition and crosslinking on the physical properties of films. The higher roughness of collagen-based films compared with gelatin-based films (Figure 3 and 4) could be attributed to the presence of larger fibre bundles in

collagen films compared with the finer scale microstructure of gelatin films (Figure 2). These collagen fibre bundles aligned in the plane of the film, giving rise to a stiffer structure compared with the gelatin, which is lacking these long, stiff fibres. The stiffness of the mixed composition film is likely to depend on the stiffness of the weakest component, and thus has properties most similar to gelatin. Those collagen fibres that are present are unlikely to be fully interconnected due to the surrounding gelatin, and thus provide limited mechanical benefit. The crosslinking process did not alter the banding structure of collagen, which had a periodicity similar to previously recorded values [32, 50], or the fibril size, but it did result in a reduced roughness. It is likely that the crosslinking process pulls fibres closer together in the formation of inter-fibre bonds and thus produces a denser, smoother structure. These inter-fibre bonds provide additional strength to the films and prevent fibre and chain sliding, therefore providing mechanical stability to the films (Figure 6).

In previous cell culture studies [34, 51], it has been shown that cells seeded on biomaterial scaffolds appear to interact with the scaffold struts, thus although it is important to establish the bulk material properties, it is equally as important to understand the properties of the scaffold a at cellular level. Previous work by others has postulated that both cell adhesion receptors and stress fibres contribute to the cellular response to the stiffness and roughness of the matrix on which they are seeded [21, 32, 52−55]. Thus the physical properties of the film, as well as the biological signals, may therefore alter cell activity and attachment to the biomaterial.

Previous research by Hafemann *et al.,* showed no significant difference in cell growth or spreading after crosslinking [12]. They studied the biocompatibility of non-/crosslinked collagen-elastin films using fibroblasts and keratinocytes. However, in our system (and additionally with HT1080 cells, unpublished results), we found that the myoblast adherent cell number and surface coverage on films was significantly reduced after crosslinking (Figure 8). This result is an agreement with recently published work by Enea *et al.* [56]. It should be noted that although crosslinking did result in a reduction in the number of adherent cells, degree of spreading of cells on films and live/dead ratio of cells, this does not necessarily indicate the inherent presence of toxic chemicals (which may be expected to produce a significantly higher number of dead cells and little live cell presence). Crosslinking reduces the cell-reactivity of films by consuming glutamate and aspartate residues (in GFOGER in collagen, or in RGD in gelatin) compared to non-crosslinked samples and the reduced live cell count or increased dead cell count may be explained by reduced initial cell

binding, where cell adhesion is required to support cell survival. Moreover, adherent cell number increased over three days in culture, indicating a reduction in adhesion rather than toxic effects of the crosslinked films.

The significant drop in cell number and coverage observed upon crosslinking is striking in that it occurs irrespective of film composition and cell type used. One interpretation of these results is that it is the increase in stiffness and reduction in roughness of the films caused by crosslinking that leads to a reduced ability for myoblasts to attach to the biomaterial. However, it should be noted that the trends reported for Young's modulus and roughness are not directly correlated to those for cell number and surface coverage when samples of different compositions are compared. For example, the gelatin films, which are weaker and smoother than collagen films, bind more cells than the pure collagen films. Furthermore, while crosslinking reduces the roughness, increases the stiffness and has a detrimental effect on the cell surface coverage on all films, the effect of crosslinking on the degree of cell spreading (as evidenced by cell area and aspect ratio) is dependent on the film composition. These comparisons suggest that although an increased stiffness and reduced roughness may cause a reduction in the adhesion of myoblast cells on films, the cell interaction (including spreading) is also highly dependent on the compositions and hence the availability and type of cell binding sites. The crosslinking process may result in a re-organisation of the fibrils and rearrangement of the cell binding sites, restricting their availability and thus resulting in the observed reduced cell surface coverage for all crosslinked films. Interestingly, whilst crosslinking collagen films results in a reduced degree of spreading (since the cell area and aspect ratio decreases) crosslinking gelatin films results in no significant difference. The GXOGEX' collagen sequences may be affected to a different extent by the crosslinking process than the RGD-cell binding sites in gelatin, so as to influence cell spreading more strongly than cell proliferation (cell number).

Gelatin films supported a higher cell count and surface coverage than collagen films for both C2C12 and C2C12-α2+ cells. Davis *et al.* and Elliot *et al.* have shown similar results in their studies of native and denatured collagen [20, 21]. Davis *et al.* showed that the adhesion of melanoma cells to native collagen type I was mediated by several β_1 integrins, including $\alpha_2\beta_1$, as well as some $\alpha_V\beta_3$. Cells adhered to denatured collagen through $\alpha_V\beta_3$ integrins, with further effects attributed to β_1, and this interaction was inhibited by RGD-containing peptides [20]. Although these studies were conducted with melanoma cells, the real-time adhesion assay results for myoblast cells presented in our paper (Figure 10) are in agreement with their

data. The assay showed an activatory response by the α2-positive cells to the type I collagen-peptide GFOGER, whereas the parent cell (which does not express specific collagen-binding integrins) did not. Furthermore, the binding of both cell lines to gelatin was shown to be RGD-dependent and relied on the presence of β_3-integrins, since blocking with anti-β_3 antibody and cyclic-RGD inhibited binding to the gelatin-coated wells. The RGD adhesion motifs in gelatin samples are more accessible than in collagen, which allows interaction with their complementary receptors on both the C2C12 and C2C12-α2+ cells, and thus increased binding of myoblast cells to gelatin compared with collagen. The triple-helical conformation of collagen fibres reduces the accessibility of the RGD motifs [20-22], but unfolding of the collagen triple helix reveals up to three copies of accessible, linear RGD for each occurrence of the motif in its primary sequence, whilst disrupting every $\alpha_2\beta_1$-binding motif such as GFOGER and related sequences for which triple-helical conformation is essential [17]. It is interesting that although the mixed film has intermediate roughness, a stiffness more similar to gelatin and should contain both the cell interaction sites that collagen and gelatin possess, it has the lowest surface coverage of cells of the three compositions studied but similar cell spreading to pure collagen films. We would expect the combination of collagen and gelatin to retain a higher number of cell binding sites; this is a result that requires further investigation.

A final comparison between cell count of films seeded with C2C12-α2+ and C2C12 myoblast cell lines was made to further establish if the biochemical interactions were integrin specific. C2C12-α2+ cells express the additional, collagen-specific integrin $\alpha_2\beta_1$, whilst parental C2C12 cells lack all collagen-binding integrins [26-28]. The α2-positive cells showed a higher cell count on collagen films than the parent cell line, but no significant difference in cell density was seen between cell types seeded on gelatin-containing films. The increased interaction of C2C12-α2+ cells with collagen compared with C2C12 cells is due to enhanced binding of the integrin $\alpha_2\beta_1$ with the specific recognition motifs on the collagen. This was confirmed in the real-time adhesion assay where the α2-positive cells showed strong Mg^{2+}-dependent adhesion to the collagen-peptide (GFOGER) coated wells, yet the parent cell lines response did not exceed that of the EDTA-inhibited cells. This difference between cell lines is not seen on gelatin films due to the absence of recognition motifs for the integrin $\alpha_2\beta_1$: both cell lines interact with RGD sequences which are more available on the gelatin [20, 55].

Previous work has focused on the comparison of different crosslinking treatments and their effect on the cytotoxicity of the biomaterial [10-12, 14] but the majority of past work has

neglected to directly compare the properties of crosslinked with non-crosslinked films. The cell reactivity of different composition films may be affected by a combination of cell receptor sites, stiffness and roughness of the films. However, the most significant effect on the bioactivity is the crosslink status. Whilst it is clearly important to crosslink the structures to 'improve' their physical properties in terms of surface roughness and mechanical stability, this has a detrimental effect on the cell activity of the films.

5. Conclusions

It is important not only to consider the properties of bulk biomaterial scaffolds but also the properties at a cellular level. The results of this study show that changing the biochemical composition and crosslinking not only affects the physical properties, such as surface roughness and mechanical stiffness, but also alters the cell activity of the films. Gelatin films are weaker and smoother than collagen films, with the increased availability RGD sequences in gelatin films providing additional binding sites for cells compared with collagen films. Most significantly, crosslinking reduced the bioactivity of the films, irrespective of the initial composition, stiffness or roughness. This result was seen with C2C12-α2+ and C2C12 cells, despite their different integrin binding motifs. This detrimental effect of crosslinking on cell response may be due to the altered physical properties of the films as well as a reduction in the number of available cell binding sites. Crosslinking is required to provide mechanical stiffness and stability; therefore it may be advantageous to enhance the cell activity by means of adding receptor-specific peptide sequences to the film surface.

Acknowledgments

The authors would like to acknowledge Simon Griggs of the Materials Department, Cambridge, for his support with scanning electron microscopy and Peter Sharratt of the Department of Biochemistry, Cambridge for help with amino acid analysis.

The authors would like to thank the Engineering and Physical Sciences Research Council and the BHF New Horizons Grant for providing financial support to this project.

References

1. Chen Q-Z, Harding SnE, Ali NN, Lyon AR, Boccaccini AR. Biomaterials in cardiac tissue engineering: Ten years of research survey. *Mater. Sci. Eng*. 2008;59:1-37.

2. Eschenhagen T, Fink C, Remmers U, Scholz H, Wattchow J, Weil J, et al. Three-dimensional reconstitution of embryonic cardiomyocytes in a collagen matrix: a new heart muscle model system. FASEB 1997;11:683-94.

3. Fujimoto KL, Tobita K, Merryman WD, Guan J, Momoi N, Stolz DB, et al. An Elastic, Biodegradable Cardiac Patch Induces Contractile Smooth Muscle and Improves Cardiac Remodeling and Function in Subacute Myocardial Infarction. *J. Am. Coll. Cardiol* 2007;49:2292-300.

4. Lee CH, Singla A, Lee Y. Biomedical applications of collagen. *Int. J. Pharm.* 2001;221:1-22.

5. Xiang Z, Liao R, Kelly MS, Spector M. Collagen–GAG Scaffolds Grafted onto Myocardial Infarcts in a Rat Model: A Delivery Vehicle for Mesenchymal Stem Cells. *Tissue Eng.* 2006;12:2467-78.

6. Chiu LLY, Radisic M, Vunjak-Novakovic G. Bioactive Scaffolds for Engineering Vascularized Cardiac Tissues. Macromol. Biosci. 2010;10:1286-301.

7. Daamen WF, Nillesen STM, Hafmans T, Veerkamp JH, van Luyn MJA, van Kuppevelt TH. Tissue response of defined collagen-elastin scaffolds in young and adult rats with special attention to calcification. Biomaterials 2005;26:81-92.

8. Eschenhagen T, Didie M, Munzel F, Schubert P, Schneiderbanger K, WH. Z. 3D Engineered heart tissue for replacement therapy. *Basic Res. Cardiol* 2002;97:146-52.

9. Harley BAC, Gibson LJ. In vivo and in vitro applications of collagen-GAG scaffolds. *Chem. Eng*. J. 2008;137:102-21.

10. Lammers G, Tjabringa GS, Schalkwijk J, Daamen WF, van Kuppevelt TH. A molecularly defined array based on native fibrillar collagen for the assessment of skin tissue engineering biomaterials. Biomaterials 2009;30:6213-20.

11. Wachem PB, van Luyn MJA, Olde Damink LHH, Dijkstra PJ, Feijen J, Nieuwenhuis P. Biocompatibility and tissue regenerating capacity of crosslinked dermal sheep collagen. *J. Biomed. Mater. Res.* 1994;28:353-63.

12. Hafemann B, Ghofrani K, Gattner HG, Stieve H, Pallua N. Cross-linking by 1-ethyl-3- (3-dimethylaminopropyl)-carbodiimide (EDC) of a collagen/elastin membrane meant to be used as a dermal substitute: effects on physical, biochemical and biological features in vitro. *J. Mater. Sci.: Mater. Med.* 2001;12:437-46.

13. Takahashi K, Nakata Y, Someya K, Hattori M. Improvement of the Physical Properties of Pepsin-Solubilized Elastin-Collagen Film by Crosslinking. *Biosci. Biotechnol. Biochem.* 1999;63:2144-9.

14. Haugh MG, Murphy CM, McKiernan RC, Altenbuchner C, O'Brien FJ. Crosslinking and Mechanical Properties Significantly Influence Cell Attachment, Proliferation, and Migration Within Collagen Glycosaminoglycan Scaffolds. Tissue Eng. 2010;17:1201-8.

15. Madhavan K, Belchenko D, Motta A, Tan W. Evaluation of composition and crosslinking effects on collagen-based composite constructs. Acta Biomater. 2010;6:1413-22.

16. Gardner JM, Hynes RO. Interaction of fibronectin with its receptor on platelets. Cell 1985;42:439-48.

17. Knight CG, Morton LF, Peachey AR, Tuckwell DS, Farndale RW, Barnes MJ. The Collagen-binding A-domains of Integrins α1β1 and α2β1 Recognize the Same Specific Amino Acid Sequence, GFOGER, in Native (Triple-helical) Collagens. *J. Biol. Chem*. 2000;275:35-40.

18. Kozlov PV, Burdygina GI. The structure and properties of solid gelatin and the principles of their modification. Polymer 1983;24:651-66.

19. Gelatin. Available from: http://www1.lsbu.ac.uk/water/hygel.html. Accessed 14-12-11.

20. Davis GE. Affinity of integrins for damaged extracellular matrix: avB3 binds to denatured collagen type I through RGD sites. *Biochem. Biophys. Res. Comm.* 1992;182:1025-31.

21. Elliott JT, Tona A, Woodward JT, Jones PL, Plant AL. Thin Films of Collagen Affect Smooth Muscle Cell Morphology. Langmuir 2002;19:1506-14.

22. Zaman MH. Understanding the Molecular Basis for Differential Binding of Integrins to Collagen and Gelatin. Biophys. J. 2007;92:L17-L9.

23. Siljander PR-M, Hamaia S, Peachey AR, Slatter DA, Smethurst PA, Ouwehand WH, et al. Integrin Activation State Determines Selectivity for Novel Recognition Sites in Fibrillar Collagens. *J. Biol. Chem*. 2004;279:47763-72.

24. Tuckwell DS, Ayad S, Grant ME, Takigawa M, Humphries MJ. Conformation dependence of integrin-type II collagen binding. Inability of collagen peptides to support alpha 2 beta 1 binding, and mediation of adhesion to denatured collagen by a novel alpha 5 beta 1-fibronectin bridge. J. Cell Sci. 1994;107:993-1005.

25. Barczyk M, Carracedo S, Gullberg D. Integrins. *Cell Tissue Res.* 2010;339:269-80.

26. Liu H, Niu A, Chen S-E, Li Y-P. B3-Integrin mediates satellite cell differentiation in regenerating mouse muscle. FASEB 2011;25:1914-21.

27. Caswell CC, Barczyk M, Keene DR, Lukomska E, Gullberg DE, Lukomski S. Identification of the First Prokaryotic Collagen Sequence Motif That Mediates Binding to Human Collagen Receptors, Integrins a2B1 and a11B1. *J. Biol. Chem*. 2008;283:36168-75.

28. Tiger C-F, Fougerousse F, Grundstrom G, Velling T, Gullberg D. alpha11beta1 Integrin Is a Receptor for Interstitial Collagens Involved in Cell Migration and Collagen Reorganization on Mesenchymal Nonmuscle Cells. Dev. Biol. 2001;237:116-29.

29. Dey S, Pal S. Evaluation of Collagen-hydroxyapatite Scaffold for Bone Tissue Engineering. IFMBE: Springer Berlin; 2009. p. 1267-70.

30. Lee SB, Kim YH, Chong MS, Hong SH, Lee YM. Study of gelatin-containing artificial skin V: fabrication of gelatin scaffolds using a salt-leaching method. Biomaterials 2005;26:1961-8.

31. Rohanizadeh R, Swain M, Mason R. Gelatin sponges (Gelfoam ®) as a scaffold for osteoblasts. *J. Mater. Sci.: Mater. Med.* 2008;19:1173-82.

32. Chung K-H, Bhadriraju K, Spurlin TA, Cook RF, Plant AL. Nanomechanical Properties of Thin Films of Type I Collagen Fibrils. Langmuir 2010;26:3629-36.

33. Olde Damink LHH, Dijkstra PJ, van Luyn MJA, van Wachem PB, Nieuwenhuis P, Feijen J. Cross-linking of dermal sheep collagen using a water-soluble carbodiimide. Biomaterials 1996;17:765-73.

34. Buttafoco L, Engbers B, Poot AA, Dijkstra PJ, Daamen WF, Kuppevelt, et al. First Steps Towards Tissue Engineering of Small-Diameter Blood Vessels: Preparation of Flat Scaffolds of Collagen and Elastin by Means of Freeze Drying. *J. Biomed. Mater. Res.* 2005;77B:357-68.

35. Ofner IIICM, Bubnis WA. Chemical and Swelling Evaluations of Amino Group Crosslinking in Gelatin and Modified Gelatin Matrices. Pharma. Res. 1996;13:1821-7.

36. Sashidhar RB, Capoor AK, Ramana D. Quantitation of [epsilon]-amino group using amino acids as reference standards by trinitrobenzene sulfonic acid: A simple spectrophotometric method for the estimation of hapten to carrier protein ratio. J. Immunol. Meth. 1994;167:121-7.

37. Horcas I, Fernandez R, Gomez-Rodriguez JM, Colchero J, Gomez-Herrero J, Baro AM. WSXM: A software for scanning probe microscopy and a tool for nanotechnology. *Rev. Sci. Instrum.* 2007;78.

38. Roche Diagnostics GmbH. Real-time and Dynamic Monitoring of Cell Proliferation and Viability for Adherent Cells. xCELLigence System: Application Note, No.1. Germany: Roche Diagnostics GmbH; 2008.

39. Castillo-Briceno P, Bihan D, Nilges M, Hamaia S, Meseguer J, Garcia-Ayala A, Farndale R *et al*. A role for specific collagen motifs during wound healing and inflammatory response of fibroblasts in the teleost fish gilthead seabream. Mol Immunol. 2011;48:826-34.

40. Jarvis G, Bihan D, Hamaia S, Pugh N, Ghevaert C, Pearce A, Hughes C *et al*. A role for adhesion and degranulation-promoting adapter protein in collagen-induced platelet activation mediated via integrin a2b1. J Thromb Haemost. 2011;10:268-77.

41. Raynal N, Hamaia SW, Siljander PR-M, Maddox B, Peachey AR, Fernandez R, Foley L *et al*. Use of Synthetic Peptides to Locate Novel Integrin {alpha}2beta1-binding Motifs in Human Collagen III. J Biol Chem. 2006;281:3821-31.

42. Smethurst PA, Onley DJ, Jarvis GE, O'Connor MN, Knight CG, Herr AB, Ouwehand W *et al*. Structural Basis for the Platelet-Collagen Interaction. J Biol Chem. 2007;282:1296-304.

43. Jorge-Herrero E, Fernandez P, Turnay J, Olmo N, Calero P, Garcia R, et al. Influence of different chemical cross-linking treatments on the properties of bovine pericardium and collagen. Biomaterials 1999;20:539-45.

44. Buttafoco L, Kolkman NG, Engbers-Buijtenhuijs P, Poot AA, Dijkstra PJ, Vermes I, et al. Electrospinning of collagen and elastin for tissue engineering applications. Biomaterials 2006;27:724-34.

45. Kale R, Bajaj A. Ultraviolet Spectrophotometric Method for Determination of Gelatin Crosslinking in the Presence of Amino Groups. *J. Young Pharmacists* 2010;2:90-4.

46. Nam K, Kimura T, Kishida A. Controlling Coupling Reaction of EDC and NHS for Preparation of Collagen Gels Using Ethanol/Water Co-Solvent. Macromol. Biosci. 2007;8:32-7.

47. Olde Damink LHH, Dijkstra PJ, Luyn MJA, Wachem PB, Nieuwenhuis P, Feijen J. Glutaraldehyde as a crosslinking agent for collagen-based biomaterials. *J. Mater. Sci.: Mater. Med*. 1995;6:460-72.

48. Powell HM, Boyce ST. EDC cross-linking improves skin substitute strength and stability. Biomaterials 2006;27:5821-7.

49. Ratanavaraporn J, Damrongsakkul S, Sanchavanakit N, Banaprasert T, Kanokpanont S. Comparison of Gelatin and Collagen Scaffolds for Fibroblast Cell Culture. *J. Met. Mat. Min*. 2006;16:31-6.

50. Fratzl P. Collagen: Structure and Mechanics, an Introduction: Springer US; 2008.

51. Freyman TM, Yannas IV, Pek YS, Yokoo R, Gibson LJ. Micromechanics of Fibroblast Contraction of a Collagen-GAG Matrix. *Exp. Cell Res.* 2001;269:140-53.

52. Yeung T, Georges PC, Flanagan LA, Marg B, Ortiz M, Funaki M, et al. Effects of substrate stiffness on cell morphology, cytoskeletal structure, and adhesion. *Cell Motility Cytoskel*. 2005;60:24-34.

53. Engler AJ, Sen S, Sweeney HL, Discher DE. Matrix Elasticity Directs Stem Cell Lineage Specification. Cell 2006;126:677-89.

54. Thomas WE, Discher DE, Shastri VP. Mechanical Regulation of Cells by Materials and Tissues. MRS Bulletin 2010;35:578-83.

55. Plant AL, Bhadriraju K, Spurlin TA, Elliott JT. Cell response to matrix mechanics: Focus on collagen. *Biochim. Biophys. Acta* 2009;1793:893-902.

56. Enea D, Henson F, Kew S, Wardale J, Getgood A, Brooks R, Rushton N. Extruded collagen fibres for tissue engineering applications: effect of crosslinking method on mechanical and biological properties. *J Mater Sci Mater Med* 2011;22:1569-1578.

Figure Captions

Figure 1. Tensile testing set up: the load cell is connected to the grips via a pulley system. Both grips and film are fully submerged. Scale bar 25 mm.

Table 1. Number of moles of free amine groups per gram of film (x 10^5) in non- and crosslinked films and calculated degree of crosslinking. Results are mean ± standard error measurement.

Figure 2. Effect of composition on film microstructure. FEGSEM images of non-crosslinked collagen and gelatin films.

Figure 3. Effect of composition and crosslinking on root mean squared roughness (R, μm) of Coll, Coll-Gel and Gel films (nX non-crosslinked, XL crosslinked). Note: * indicates statistically significant difference in comparison to non-crosslinked sample of same composition, ■ indicates statistically significant difference between compositions for statistical significance of $p \leq 0.05$ in Student's *t*-test. The error bars indicate the standard error of the mean.

Figure 4. Effect of film composition and crosslinking on surface roughness and height as measured by AFM topography images of Coll, Coll-Gel and Gel films (nX non-crosslinked, XL crosslinked).

Figure 5. Periodic banding structure of collagen fibres within the film as measured from AFM amplitude image: alternating dark and light bands indicate regions of variation of topography and the periodic repeat was measured along the straight line between the two cross-points as 64.4 ± 2.91 nm. The graph shows the change in topography between the two cross-points, and acts as a graphical representation of the banding pattern.

Figure 6. Effect of composition and crosslinking on the Young's modulus of films at different strains (5%, 20% and high strain: in the linear region of the stress-strain curve, nX non-crosslinked, XL crosslinked). Non-crosslinked films were weak when hydrated and only Coll nX was able to be tested. Note: * indicates statistically significant difference in comparison to non-crosslinked sample of same composition, ■ indicates statistically significant difference between compositions for statistical significance of $p \leq 0.05$ in Student's *t*-test. The error bars indicate the standard error of the mean.

Figure 7. Phase contrast images (a and d) and immunofluorescence images showing staining for live (Hoechst, b and e) and dead (Propidium Iodide, c and f) C2C12-α2+ cells after culture for 72 h on gelatin films of different crosslink status. (a-c) Gel nX, (d-f) Gel XL. Scale bar is 100 μm.

Figure 8. Effect of film composition and crosslinking on live cell count (a), surface coverage (c), cell area (μm^2, b) and aspect ratio (d), for C2C12-α2+ cells after 72 h culture. Note: * indicates statistically significant difference in comparison to non-crosslinked sample of same composition, ■ indicates statistically significant difference between collagen-based and gelatin-based films for statistical significance of $p \leq 0.05$ in two-way ANOVA. The error bars indicate the standard error of the mean.

Figure 9. Effect of film composition and crosslinking on cell count of a) C2C12-α2+ and b) C2C12 cells after 72 h culture. Note: * indicates statistically significant difference in comparison to non-crosslinked sample of same composition, ■ indicates statistically significant difference between cell lines (C2C12 and C2C12-α2+) for statistical significance of $p \leq 0.05$ in two-way ANOVA. The error bars indicate the standard error of the mean.

Figure 10. Real time adhesion and spreading of a) C2C12 and C2C12-α2+ cells to GFOGER peptide (10 μg/ml) and b) C2C12 cells or c) C2C12-α2+ cells to gelatin (100 μg/ml). In b) and c) cells were blocked by pre-incubation with cyclic-RGD (c-RGD) or anti-β3 integrin (anti-β3). Incubations were carried out in the presence of 1 mM Mg^{2+}, to enhance, or EDTA, to inhibit the integrin-mediated cell binding. The xCELLigence system measured impedance every 30 s, reported as cell index value. Lines represent mean (standard error measurements not significant) for n = 6. Different conditions denoted with shaped markers.

Figures

Figure 1.

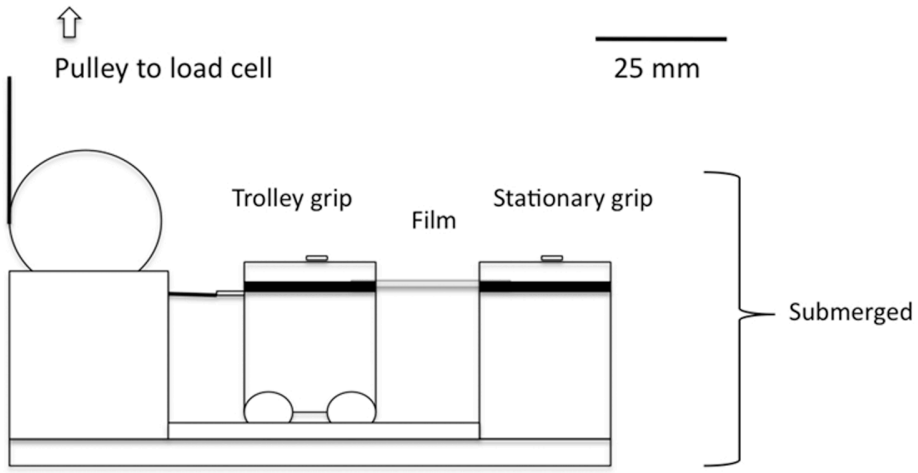

Table 1.

	Non-crosslinked	Crosslinked	Degree of Crosslinking
Coll	14 ± 2.8	7.3 ± 1.4	0.49 ± 0.14
Coll-Gel	25 ± 5.8	8.7 ± 1.9	0.66 ± 0.04
Gel	23 ± 14	4.2 ± 2.3	0.82 ± 0.06

Figure 2.

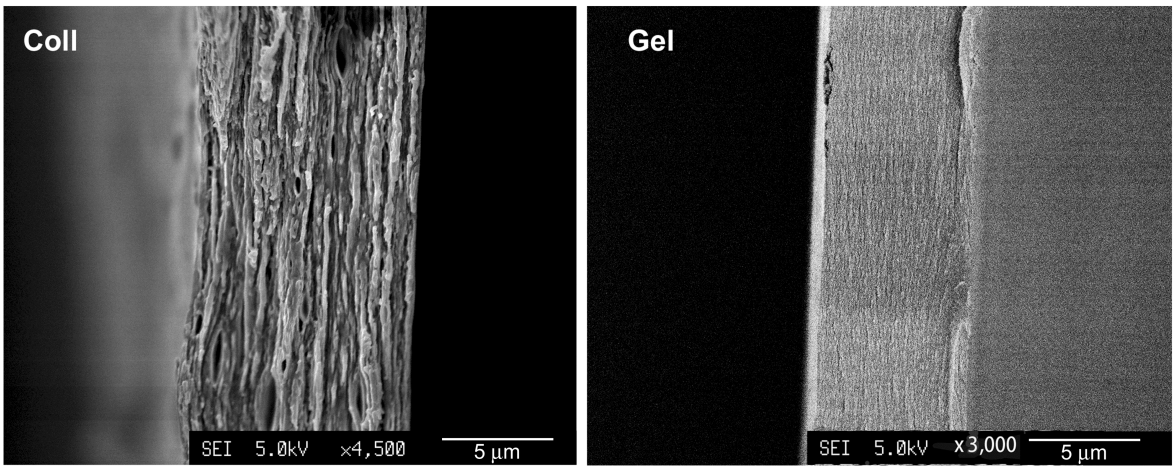

Figure 3.

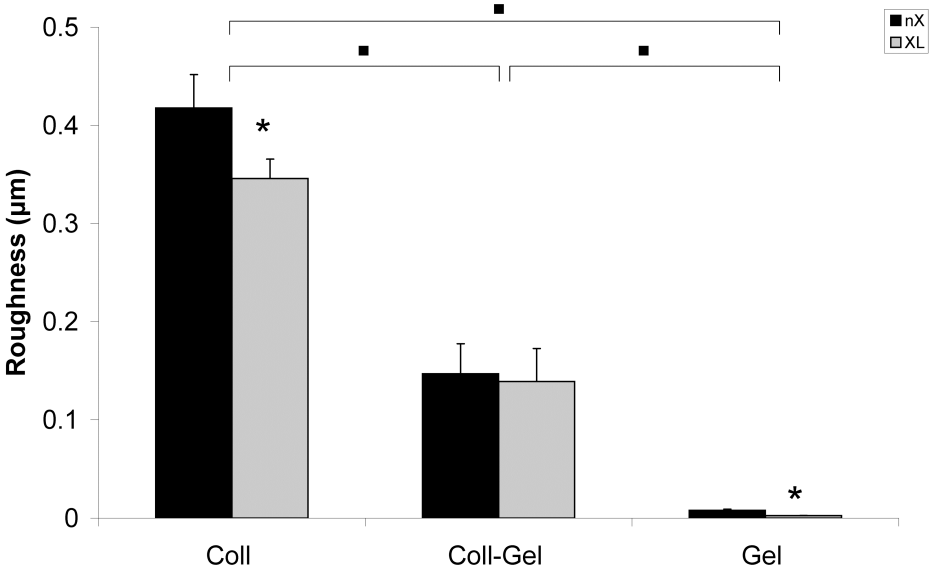

Figure 4.

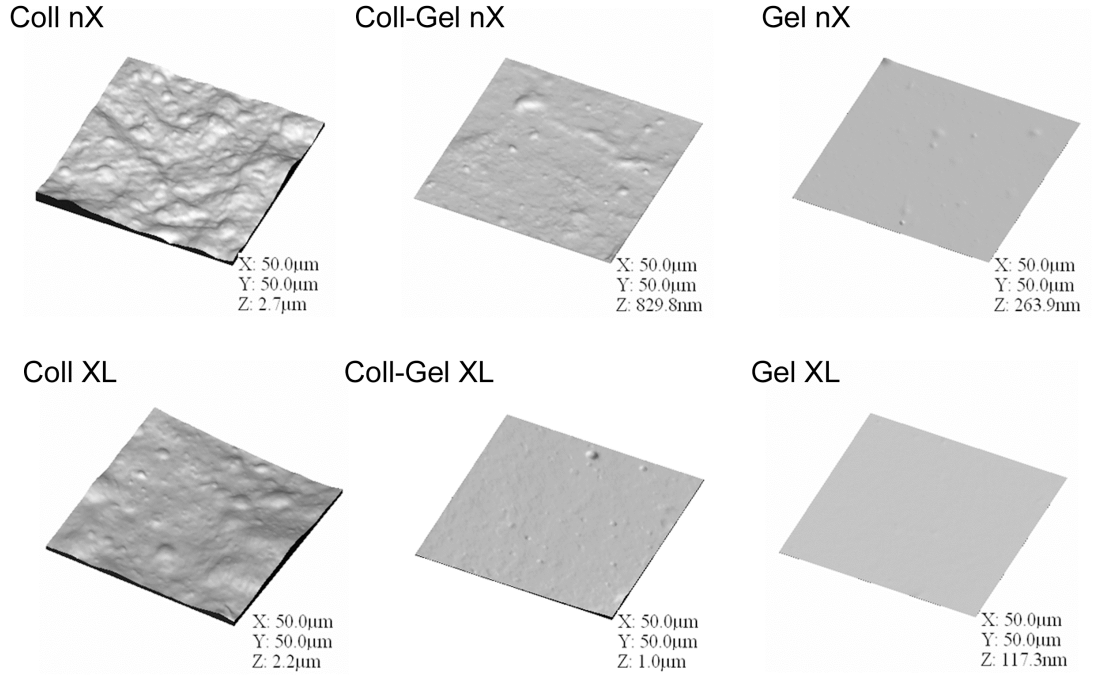

Figure 5.

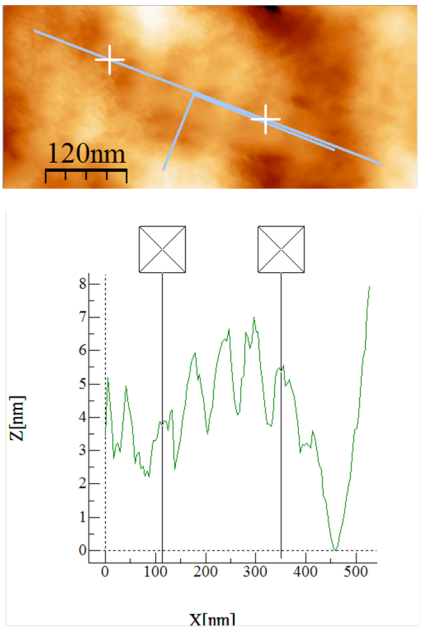

Figure 6.

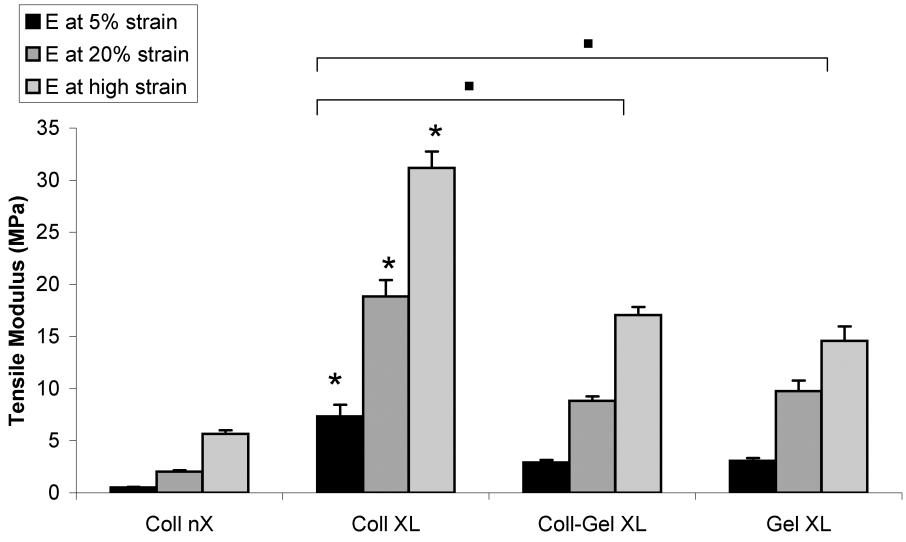

Figure 7.

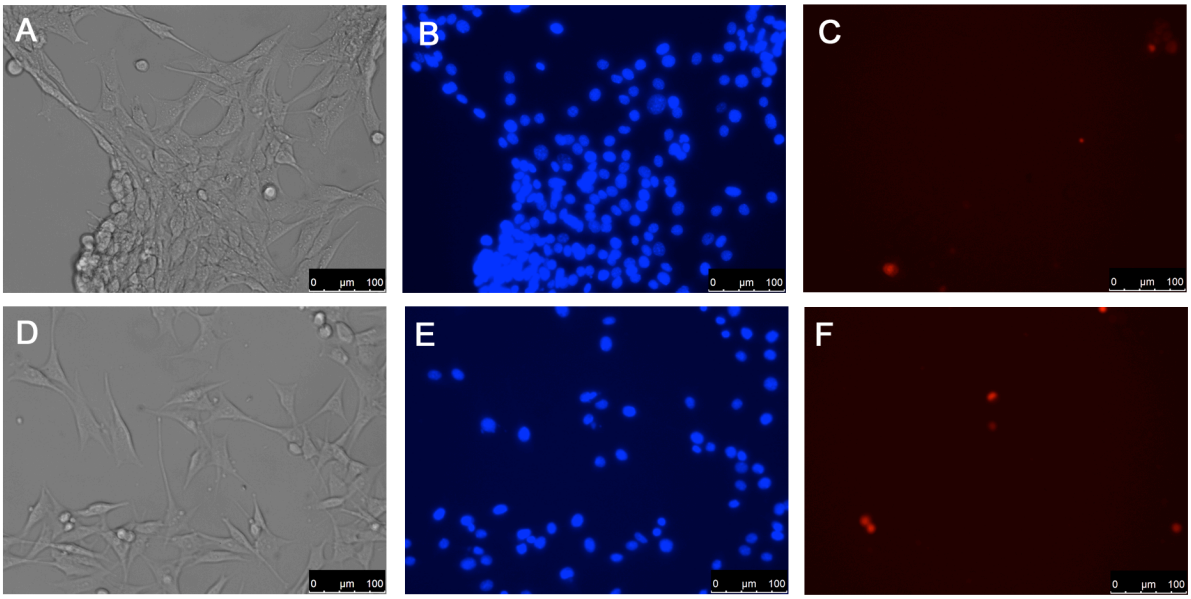

Figure 8.

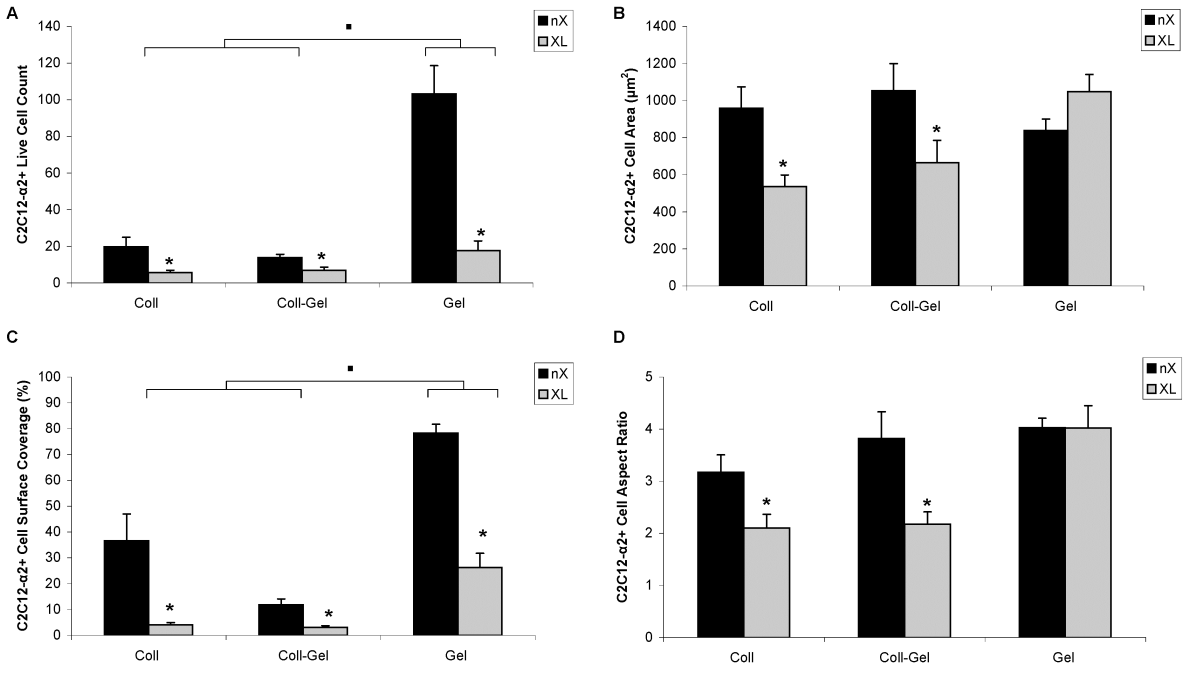

Figure 9.

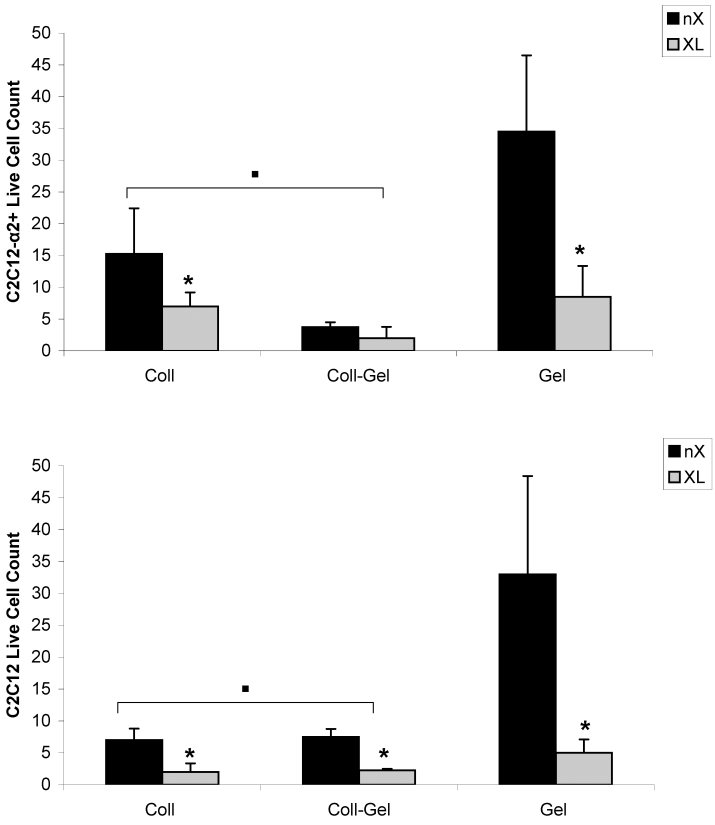
nX
XL
C2C12-α2+ Live Cell Count
50
45
40
35
30
25
20
15
10
5
0
Coll
Coll-Gel
Gel
nX
XL
C2C12 Live Cell Count
50
45
40
35
30
25
20
15
10
5
0
Coll
Coll-Gel
Gel

Figure 10.

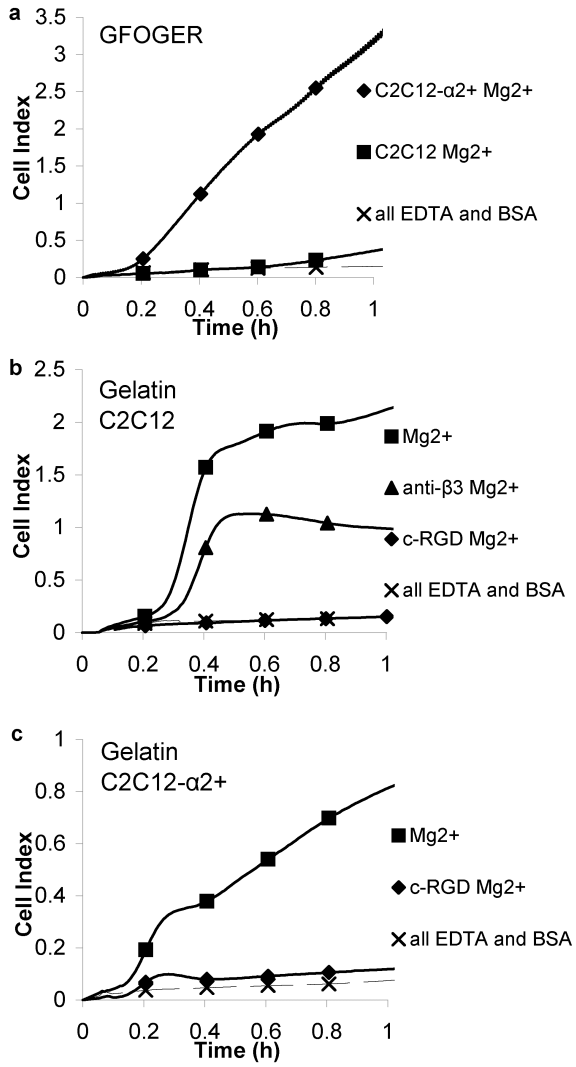
a
GFOGER
Cell Index
Time (h)
C2C12-α2+ Mg2+
C2C12 Mg2+
all EDTA and BSA
b
Gelatin
C2C12
Cell Index
Time (h)
Mg2+
anti-β3 Mg2+
c-RGD Mg2+
all EDTA and BSA
c
Gelatin
C2C12-α2+
Cell Index
Time (h)
Mg2+
c-RGD Mg2+
all EDTA and BSA